Artificial Magnetic Conductors Realized by Planar Array of Loaded Loop for Antenna Applications

SeyedMohammad Hashemi, Student Member IEEE, Mohammad Soleimani,
Department of Electrical Engineering,
Iran University of Science and Technology,
Tehran 1684613114, Iran
E-mail: hashemy@iust.ac.ir, Soleimani@iust.ac.ir.

***Abstract*—New designs of artificial magnetic conductors (AMC), including dual-polarized and multiband AMC are realized by planar regular array of loaded loop over a ground surface. Multiband designs of AMC surfaces are proposed based on the use of loaded loop with different resonance lengths. In addition, dual-polarized AMC are realized by loops with different orientation, which create artificial magnetic conductors for both TE and TM polarizations. The approximate analytical models were developed to estimate the AMC surface response. FEKO electromagnetic simulator is also used for the fullwave analysis of presented configurations.**

Keywords- artificial magnetic conductors; loaded loop; dual-polarized AMC; multiband AMC;

I. Introduction

Since the introduction of high impedance surfaces (HIS) or artificial magnetic conductors (AMC) in [1], many researchers have used them to design novel electromagnetic devices or enhance the performance of the existing ones. The features of these surfaces have resulted in many novel and improved applications such as quasi-TEM [2] and impedance waveguides [3], [4], bandgap structures [5], low-profile antennas [6], [7], leaky-wave antennas [8], [9], and absorbers [10], [11].

Different approaches have been used for the realization of AMC surfaces. They are realized by metal patches on the top surface of the board, connected to the solid lower conducting surface by metal plated vias in [1]. The metal patches may have various shapes and its effects investigated in [12]. Another method is to realize them by printed dipoles on a grounded dielectric slab which Multiband/dual-polarized designs are discussed in [13], [14]. One other method is volumetric realization that does not require a ground plane. The capacitively-loaded loop (CLL) based slab which exhibit AMC properties and two reversed Ω patterns back to back on each side of a substrate board presented in [15] and [16] respectively.

Here we introduce an AMC surfaces that are composed of loaded loop in planar manner. The unit cell of this periodic structure is illustrated in Fig. 1. The loop lay in the *xy*-plane and load is on *X*-axis. The *"a"* and *"w"* are inner dimension and width of loop respectively and *"d"* is dimension of the unit cell. A closed loop (or simply a ring), a split ring and also a capacitively-loaded loop are different types of loaded loop which the loop loaded by short, open and capacitive load (Fig. 4). We consider all types of these loaded loops and discuss about the effect of each load on the reflection features of the AMC surface.

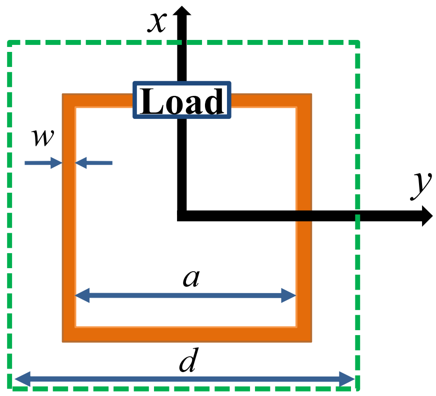

Figure 1. Loaded loop unit cell.

Subsequently, we suggest multiband unit cell based on the use of loaded loop with different resonance lengths. In this case the effect of different orientations for each loop on the AMC surface response will be checked. Since the loaded loop is not symmetric, the AMC surface which is made of them is not dual-polarized at least in the same frequency. We also discuss about arrangement of loaded loop for realization of dual-polarized AMC surface.

II. Planar Array of Loaded Loop

Consider a regular plane square array with period *"d"* formed by passive lossless scatterers located near an ideally conducting plane and parallel to that plane. The distance between the array plane and the ground plane is *"h"*. Let us consider the case of an array formed by nearly resonant electric dipoles. We assume the normal plane-wave incidence, to simplify the analysis and choose the coordinate system with the zero-point in the center of one reference scatterers, with the *Z*-axis normal to the ground plane and *X*, *Y*-axes parallel to the sides of the elementary cell as at Fig. 2. The reflection coefficient from the structure is equal to [17]:

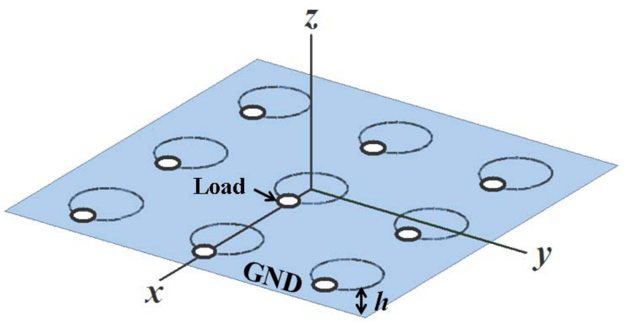

Figure 2. Planar regular array of loaded loop over a grounded dielectric slab (h=1.6 mm and ε_r=10.2).

$$R = -1 + \frac{2}{1 - j\varepsilon_0 d^2 \dfrac{\mathrm{Re}\{\alpha^{-1} - C\}}{k_0 \sin(k_0 h)}} \tag{1}$$

k_0 is the wave vector, α is the polarizability coefficient of scatterers and C is so-called interaction constant and the formulation can be found in [17], [18]. The real part of quantity C is positive. The real part of the inverse polarizability α^{-1} for small conducting particles is also positive, so in principle $\mathrm{Re}\{C\}$ can match the positive real part of α^{-1} [17]. The problem is that if the polarizability value is small, its inverse value is large, and it cannot be compensated by the interaction constant. In this case the reflection coefficient is close to −1. For higher polarizabilities the resonance is possible when $\mathrm{Re}\{\alpha^{-1} - C\} = 0$. The reflection coefficient becomes equal to +1 which corresponds to a magnetic surface [17].

From these considerations we see that to realize very thin resonant layers we should find a way to increase the particle polarizability without increasing its size. This can be made possible by loading particles by some loads. For example for short strip dipoles with capacitive input impedance if the load impedance is inductive, the particle polarizability near the particle resonance becomes large, which makes it possible to

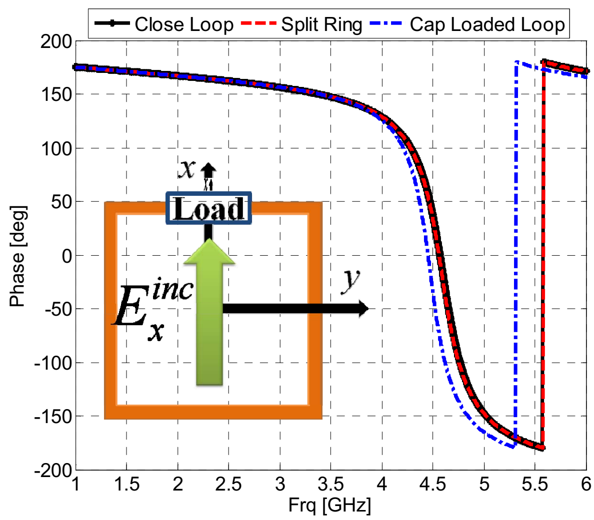

Figure 3. The reflection phase of different loaded loop (in Fig. 4) for E_x as a incident electric field polarization.

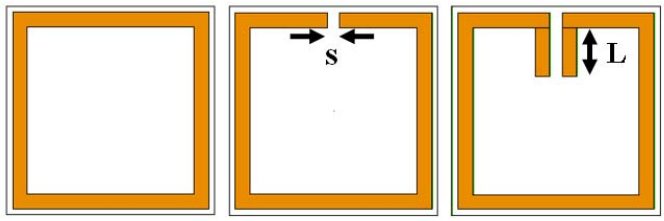

a) b) c)

Figure 4. The unit cell of different loops, s=0.3 mm, L=1.17 mm, (Fig. 1. parameters: d=5 mm, a=4 mm, w=0.35 mm).
a) Close loop, b) Split loop, c) Capacitive loaded loop.

fulfill the resonance condition for a grid over conducting plane [17].

Also for a loop which is considered here, with inductive input impedance if the load impedance is capacitive, same result can be achieved. So, the main goal is to obtain a resonance at low frequencies where the substrate thickness *"h"* is very small compared to the wavelength and the period *"d"* is also small.

A. Polarizability Of Loaded Loop

Consider a small circular loop formed by an ideally conducting wire. Let us assume that the electrical size of the loop is not large, which results in the following approximate formula for input admittance [18]:

$$Y_{loop} = \frac{-j}{\pi\eta_0}\left(\frac{1}{A_0} + \frac{2}{A_1}\right) \tag{2}$$

where A_0 and A_1 are the coefficients of Fourier series expansion of the current distribution function with respect to the polar angle φ measured around the loop.

Consider the planar regular array of loaded loop over a ground surface in Fig. 2. If the incident electric field is in the plane of the loop, the loop response depends on the orientation

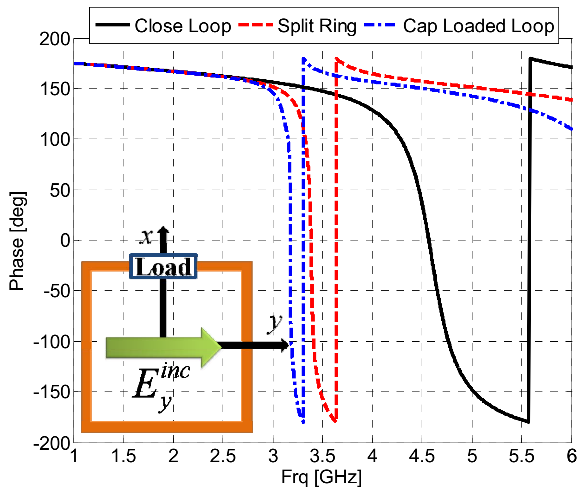

Figure 5. The reflection phase of different loaded loop (in Fig. 4) for E_y as a incident electric field polarization.

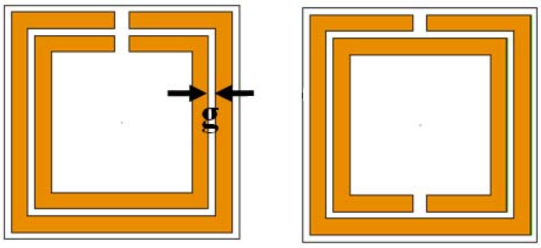

Figure 6. Multiband unit cells based on the use of loaded loop with different resonance lengths. g=0.15 mm (both ring have same "*w*" and dimensions is similar to that in Fig. 4)

of the field with respect to the position of the load. The current excited in the loop can be divided into two parts, so that one of them does not depend on the load position and coincides with that exited in a closed loop. For the case when the external electric field is polarized along the *X*-axis, this component actually represents the whole current and allows us to find the polarizability [18]:

$$\alpha_{ee}^{xx} = -\frac{4\pi a^2 J_1'(k_0 a)}{\omega \eta_0 A_1} \quad (3)$$

The second component of the current can be considered as one generated by an equivalent source located at the load position, and that component is proportional to the y-polarized of the external electric field. These currents can be calculated using the theory of loop antenna, and then the polarizability can be determined as [18]:

$$\alpha_{ee}^{yy} = -\frac{4\pi a^2 J_1'(k_0 a)}{\omega \eta_0 A_1}\left(1+\frac{2j}{\pi \eta_0 A_1}\frac{1}{Y_{loop}+Y_{load}}\right) \quad (4)$$

With these polarizability coefficients the response of surface would be estimated. If the incident electric field is polarized along the *X*-axis the load does not have significant effect on resonance frequency and the surface response is similar to closed loop (Fig. 3). But if electric field is polarized along the *Y*-axis the effect of load would be seen (Fig. 5). Also since the load impedance is capacitive if we increase the capacitance the lower resonance frequency achieved.

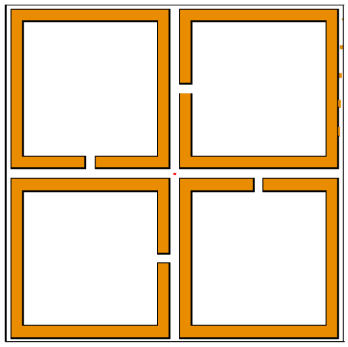

Figure 8. Arrangement of loaded loop for realization of dual-polarized AMC surface (dimensions is similar to that in Fig. 4).

Rectangular (circular) loops used in printed FSS result in dual-polarized wideband high-impedance surfaces [14]. Here, we propose to use loaded rectangular loops in order to create an AMC structure.

B. Multiband AMC

Dual-band AMC designs was importance for example where dual subreflectors were used as feeds for the main reflector operating at two desired bands. Also, it has been proposed in [13], [14] to use more than one element in a single unit cell in order to create multiband AMC surfaces. This idea is applied here in the design of dual-band AMC surfaces using printed loaded loop implemented on a grounded dielectric slab, wherein two loops of different resonance lengths are considered in a unit cell (Fig. 6).

C. Dual-polarised AMC

Since the loaded loop is not symmetric, the AMC surface which is made of them is not dual-polarized at least in the same frequency. So we can control the AMC surface response by loading the loop only for one polarization (Fig. 5). For the other polarization, the AMC surface is similar to closed loop surface and the load does not have significant effect on resonance frequency (Fig. 3). To overcome the problem we can arrange the loaded loop as illustrated in Fig. 8.

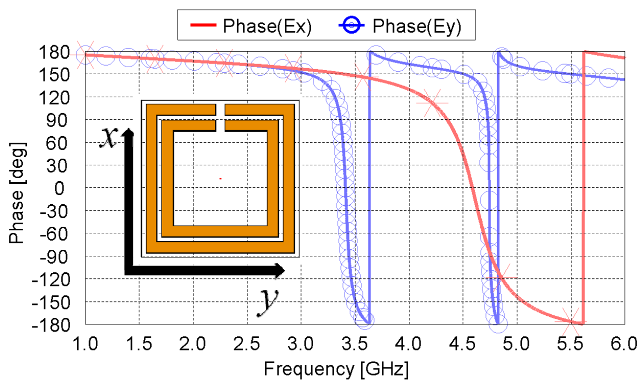

Figure 7. The reflection phase of dual-band unit cell when the position of both gaps is the same.

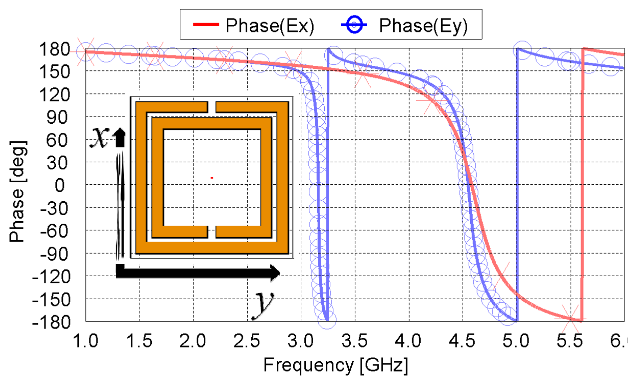

Figure 9. The reflection phase of dual-band unit cell when the position of gaps is different.

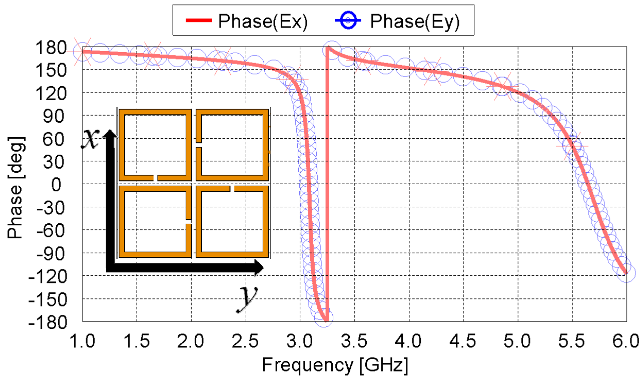

Figure 10. The reflection phase of dual-polarized arrangement (Fig. 8) of split loop for E_x and E_y polarization.

III. Simulation Results and Discussion

Here we discuss about the simulation results for these different loaded loop: closed loop, split loop, capacitive loaded loop and consider Multiband unit cells and dual-polarized arrangement. All structures are backed by a grounded dielectric slab having thickness of *h*=1.6 mm and $\varepsilon_r = 10.2$. The loaded loop unit cell parameters are: *a*=4 mm, *w*=0.35 mm, *d*=5 mm (Fig. 1). We compare the reflection phase of the different loaded loops lay in the *xy*-plane in Figs. 3 and 5. As predicted by analytical models, loading loop causes lower resonance frequency but less bandwidth. Also *x*-polarized electric field is similar to closed loop, but for the *y*-polarized electric field we have smaller zero phase reflection first frequency and if we increase the capacitance the lower resonance frequency achieved. So we can control the zero phase reflection frequency by changing the load capacitance.

We also suggest multiband unit cell based on the use of loaded loop with different resonance lengths (Fig. 6). The results are illustrated in Figs. 7 and 9. A frequency of 180^0 reflection phase occurs between the two AMC bands. For any perturbed AMC, there will always be a frequency point between the two AMC bands where the incident wave will be reflected with a phase reversal [13]. This resonance poses a fundamental limitation in the performance of multiband AMCs. Therefore a dual AMC response with the two bands in close proximity suffers from poor bandwidth performance. The bandwidth can be improved by increasing the spectral separation [13].

Any desired loaded loop unit cell can be arranged as illustrated in Fig. 8 to get same results (smaller zero phase reflection frequency) for both polarizations as illustrated in Fig. 10. So now we have dual-polarized and/or multiband smaller unit cell for every AMC applications.

Acknowledgment

The authors would like to thank the MSRT (The Ministry of Science, Research and Technology) and ITRC (Iran Telecommunication's research center) for their supports in my exchange period.

References

[1] D. Sievenpiper, Z. Lijun, R. F. J. Broas, N. G. Alexopolous, and E. Yablonovitch, “High-impedance electromagnetic surfaces with a forbidden frequency band,” Microwave Theory and Techniques, IEEE Transactions on, vol. 47, pp. 2059-2074, 1999.

[2] F.-R. Yang, K.-P. Ma, Y. Qian, and T. Itoh, “A novel TEM waveguide using uniplanar compact photonic-bandgap (UC-PBG) structure,” IEEE Trans. Microw. Theory Tech., vol. 47, no. 11, pp. 2092–2098, Nov. 1999.

[3] J. A. Higgins, H. Xin, A. Sailer, and M. Rosker, “Ka-band waveguide phase shifter using tunable electromagnetic crystal sidewalls,” IEEE Trans. Microw. Theory Tech., vol. 51, no. 4, pp. 1281–1287, Apr. 2003.

[4] O. Luukkonen, C. Simovski, A. V. Räisänen, and S. A. Tretyakov, “An efficient and simple analytical model for analysis of propagation properties in impedance waveguides,” IEEE Trans. Microw. Theory Tech., vol. 56, no. 7, pp. 1624–1632, Jul. 2008.

[5] F. Yang and Y. Rahmat-Samii, “Microstrip antennas integrated with electromagnetic band-gap (EBG) structures: A low mutual coupling design for array applications,” IEEE Trans. Antennas Propag., vol. 51, no. 10, pp. 2936–2946, Oct. 2003.

[6] A. P. Feresidis, G. Goussetis, S. Wang, and J. C. Vardaxoglou, “Artificial magnetic conductor surfaces and their application to low-profile high-gain planar antennas,” IEEE Trans. Antennas Propag., vol. 53, no. 1, pp. 209–215, Jan. 2005.

[7] J. M. Bell and M. F. Iskander, “A low-profile Archimedean spiral antenna using an EBG ground plane,” IEEE Antennas Wireless Propag. Lett., vol. 3, no. 1, pp. 223–226, 2004.

[8] D. Sievenpiper, J. Schaffner, J. J. Lee, and S. Livingston, “A steerable leaky-wave antenna using a tunable impedance ground plane,” IEEE Antennas Wireless Propag. Lett., vol. 1, no. 1, pp. 179–182, 2002.

[9] D. F. Sievenpiper, “Forward and backward leaky wave radiation with large effective aperture from an electronically tunable textured surface,” IEEE Trans. Antennas Propag., vol. 53, no. 1, pp. 236–247, Jan. 2005.

[10] N. Engheta, “Thin absorbing screens using metamaterial surfaces,” in IEEE AP-S Int. Symp. Dig., San Antonio, TX, 2002, vol. 2,, pp. 392–395.

[11] S. A. Tretyakov and S. I. Maslovski, “Thin absorbing structure for all incident angles based on the use of a high-impedance surface,” Microw. Opt. Technol. Lett., vol. 38, no. 3, pp. 175–178, 2003.

[12] A. Foroozesh and L. Shafai, “Investigation Into the Application of Artificial Magnetic Conductors to Bandwidth Broadening, Gain Enhancement and Beam Shaping of Low Profile and Conventional Monopole Antennas,” Antennas and Propagation, IEEE Transactions on, vol. 59, pp. 4-20, 2011.

[13] G. Goussetis and A. P. Feresidis, “Perturbed frequency selective surfaces for multiband high impedance surfaces," Microwaves, Antennas & Propagation, IET, vol. 4, pp. 1105-1110, 2010.

[14] Hiranandani, M. A., A. B. Yakovlev, et al. (2006). "Artificial magnetic conductors realised by frequency-selective surfaces on a grounded dielectric slab for antenna applications." Microwaves, Antennas and Propagation, IEE Proceedings - 153(5): 487-493.

[15] A. Erentok, P. L. Luljak, and R. W. Ziolkowski, “Characterization of a volumetric metamaterial realization of an artificial magnetic conductor for antenna applications," Antennas and Propagation, IEEE Transactions on, vol. 53, pp. 160-172, 2005.

[16] M. Veysi, M. Kamyab, S. M. Mousavi, and A. Jafargholi, “Wideband Miniaturized Polarization-Dependent HIS Incorporating Metamaterials," Antennas and Wireless Propagation Letters, IEEE, vol. 9, pp. 764-766, 2010.

[17] P. A. Belov and S. A. Tretyakov, "Resonant Reflection From Dipole Arrays Located Very Near To Conducting Planes," Journal of Electromagnetic Waves and Applications, vol. 16, pp. 129-143, 2002.

[18] S. Tretyakov, “Analytical Modeling in Applied Electromagnetics,” Artech House, Norwood, MA, 2003.